Universality and nonuniversality of mobility in heterogeneous single-file systems and Rouse chains

Michael A. Lomholt*
MEMPHYS-Center for Biomembrane Physics, Department of Physics, Chemistry and Pharmacy, University of Southern Denmark, Campusvej 55, DK-5230 Odense M, Denmark

Tobias Ambjörnsson
Department of Astronomy and Theoretical Physics, Lund University, Sölvegatan 14A, SE-223 62 Lund, Sweden
(Received 2 September 2013; published 3 March 2014)

We study analytically the tracer particle mobility in single-file systems with distributed friction constants. Our system serves as a prototype for nonequilibrium, heterogeneous, strongly interacting Brownian systems. The long time dynamics for such a single-file setup belongs to the same universality class as the Rouse model with dissimilar beads. The friction constants are drawn from a density $\varrho(\xi)$, and we derive an asymptotically exact solution for the mobility distribution $P[\mu_0(s)]$, where $\mu_0(s)$ is the Laplace-space mobility. If ϱ is light tailed (first moment exists), we find a self-averaging behavior: $P[\mu_0(s)] = \delta[\mu_0(s) - \mu(s)]$, with $\mu(s) \propto s^{1/2}$. When $\varrho(\xi)$ is heavy tailed, $\varrho(\xi) \simeq \xi^{-1-\alpha}$ $(0 < \alpha < 1)$ for large ξ, we obtain moments $\langle[\mu_s(0)]^n\rangle \propto s^{\beta n}$, where $\beta = 1/(1+\alpha)$ and there is no self-averaging. The results are corroborated by simulations.

DOI: 10.1103/PhysRevE.89.032101 PACS number(s): 05.40.−a, 02.50.Ey, 82.39.−k

I. INTRODUCTION

Studies of the force response properties in complex media have a long tradition in physics [1,2]. In biology, forces are involved in a large number of different processes in cells, and moreover, forces are commonly used in force probing, for instance, of macromolecular structure in *in vitro* systems [3]. The Jarzynski equality relates the time-averaged response of a system when under the influence of a force to the free energy between initial and final states [4]. Recently, an exact solution to a paradigm nonequilibrium model for homogeneous systems, the asymmetric exclusion process, was put forward [5].

In this article we provide asymptotically exact solutions for the force response of a complex *heterogeneous* system: tracer particle dynamics in a single-file system (the same universality class as harmonically coupled dissimilar beads or Rouse chains, for long times) with randomly distributed friction constants. Our model serves as a prototype for the nonequilibrium dynamics in heterogeneous, strongly interacting Brownian systems. Even for the case when all particles have identical friction constants, such systems display nontrivial dynamics characterized by a subdiffusive behavior [6–9]. Few studies have addressed the problem of the diffusion of hardcore particles with different friction constants; for undriven systems see Refs. [10–16]. Of particular interest for the present study is Ref. [16], where an effective medium approximation was applied, revealing ultraslow time evolution of the mean square displacement, and where simulations indicated lack of self-averaging. To our knowledge the problem addressed in this paper, namely, the exact force-response relation for tracer particle dynamics in single-file systems with distributed friction constants, has not been addressed previously. From our treatment of these systems we also obtain exact results for the mean square displacement of the tracer particle.

Besides its theoretically interesting properties, the single-file problem finds a number of experimental realizations: transport in microporous materials [17–19] (e.g., zeolites), colloidal systems [20], molecular sieves [21], and biological pores [22]. Cooperative effects are of importance in transport processes involving molecular motors [23,24]. Hardcore repulsion of binding proteins diffusing along DNA has been shown to be important in transcription [25].

II. DESCRIPTION OF THE SYSTEM

Let us state the problem. We consider strongly overdamped motion of Brownian particles in an infinite one-dimensional system, interacting via a two-body short-range repulsive potential. This potential, $\mathcal{V}(|x_n(t) - x_{n'}(t)|)$, where $x_n(t)$ is the position of the nth particle, has a hard-core part which excludes particles from overtaking each other. The Langevin equations of motion are thus $\xi_n \dot{x}_n(t) = \sum_{n'} \mathfrak{f}[x_n(t) - x_{n'}(t)] + \eta_n(t) + f_0(t)\delta_{n,0}$ where a dot denotes the time derivative, $\mathfrak{f} = -\partial\mathcal{V}/\partial x_n$ is the interaction force, $\eta_n(t)$ is a Gaussian zero-mean noise, $< \eta_n(t) >= 0$, with correlations that are related to the friction constants ξ_n by the fluctuation-dissipation theorem [26] as $< \eta_n(t)\eta_{n'}(t') >= 2k_BT\xi_n\delta(t-t')\delta_{n,n'}$, where k_B is the Boltzmann constant and T is the temperature. $f_0(t)$ is an external force acting only on particle 0 (the tracer particle). In our simulations we take $f_0(t)$ to be an oscillating force. A cartoon of the problem at hand is depicted in Fig. 1.

As was shown in [16,27] using a *harmonization* approach, the long time limit of the Langevin equation above with a sufficiently small external force $f_0(t)$ is the same as that for a linear chain of interconnected springs,

$$\xi_n \frac{dx_n(t)}{dt} = \kappa\,[x_{n+1}(t) + x_{n-1}(t) - 2x_n(t)] + \eta_n(t) + f_0(t)\delta_{n,0}. \quad (1)$$

The effective nearest neighbor spring constant κ is obtained from the system's equation of state. For hard-core interacting

*mlomholt@memphys.sdu.dk

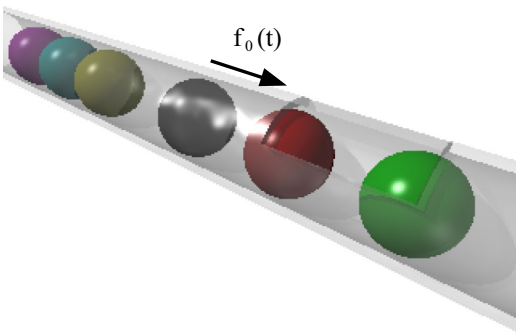

FIG. 1. (Color online) Cartoon of the heterogeneous single-file system investigated in this article. Dissimilar hardcore interacting particles (the particles cannot overtake) are diffusing in a one-dimensional system. The particles are assigned *different* friction constants ξ_n (n labels different beads), drawn from a probability density $\varrho(\xi_n)$. A time-varying force, $f_0(t)$, acts on a tracer particle (colored black). In such a scenario we study the tracer particle force response properties through the mobility defined in Eq. (3).

particles of size b (used in our simulations) this harmonization procedure yields [27] $\kappa = \rho^2 k_B T(1-\rho b)^{-2}$, where ρ is the particle density.

The heterogeneity of the particles enters through their different friction constants ξ_n, which here are assumed to be identically distributed random variables taken from a probability density $\varrho(\xi_n)$. We distinguish between light-tailed (LT) distributions for which the mean $\bar{\xi}$ of $\varrho(\xi)$ exists and heavy-tailed (HT) systems, where

$$\varrho(\xi) \sim A\xi^{-1-\alpha} \tag{2}$$

for large ξ, with A being a constant prefactor and $0 < \alpha < 1$ such that the mean diverges.

The main quantity of interest in this study is the distribution $P[\hat{\mu}_0(s)]$ of mobilities of tracer particle 0 defined as (in the Laplace domain)

$$\hat{\mu}_0(s) \equiv \frac{<\hat{v}_0(s)>}{\hat{f}_0(s)}, \tag{3}$$

where $v_0(t) = dx_0(t)/dt$ is the tracer particle velocity and we use a hat to distinguish quantities in Laplace space [Laplace-transforms are defined as $\hat{A}(s) = \int_0^\infty dt\, e^{-st} A(t)$]. The $<\cdots>$ brackets represent an average over different realizations of the thermal noise and random initial positions. We label this average the *nonaveraged* case. It is contrasted by the *heterogeneity-averaged* case (represented by $\langle\cdots\rangle$), where an additional average over the probability density of friction constants is performed. In the simulations for the nonaveraged case the same ξ_n's are used when averaging over thermal noise (i.e., for each simulation run). For the heterogeneity-averaged case we draw new friction constants whenever we make a new initial particle positioning.

Turning back to Eq. (1), introducing the quantity $y_n(t) = x_n(t) - n/\rho$ and taking the Laplace transform, we obtain

$$\xi_n[s<\hat{y}_n(s)> - <y_n(0)>] = \kappa[<\hat{y}_{n+1}(s)> + <\hat{y}_{n-1}(s)> - 2<\hat{y}_n(s)>] + \hat{f}_0(s)\delta_{n,0}. \tag{4}$$

We proceed by introducing the quantities $m_n^{(\pm)}$, representing the mobility of the chain to the right (+) or left (−) starting from particle n (using $<y_n(0)> = 0$), defined as

$$m_n^{(\pm)}(s) = \frac{s<\hat{y}_n(s)>}{-\kappa[<\hat{y}_n(s)> - <\hat{y}_{n\mp1}(s)>]}. \tag{5}$$

Notice that the denominator represents the velocity of particle n, while the numerator represents the force from one of its harmonic springs. With these definitions we obtain the following expression for the tracer particle mobility of particle 0 [28]:

$$\hat{\mu}_0(s) = \left(\xi_0 + \frac{1}{s/\kappa + m_1^{(+)}(s)} + \frac{1}{s/\kappa + m_{-1}^{(-)}(s)}\right)^{-1}, \tag{6}$$

as well as the following recurrence relations:

$$m_{\pm n}^{(\pm)}(s) = \left(\xi_n + \frac{1}{s/\kappa + m_{\pm(n+1)}^{(\pm)}(s)}\right)^{-1}, \quad n > 0. \tag{7}$$

For a given set of ξ_n's, Eqs. (6) and (7) provide an exact expression for the tracer particle mobility in the non-averaged case.

III. TRACER MOBILITY FOR ξ_n BEING INDEPENDENT, IDENTICALLY DISTRIBUTED RANDOM VARIABLES

We now proceed to consider heterogeneity averages by assuming that the ξ_n's are independent, identically distributed (iid) random numbers and try to solve Eqs. (6) and (7) for the probability distribution of $\hat{\mu}_0(s)$. Note that since the ξ_n's are identically distributed random variables, so are the m_n's; we denote by $g_s(m_n)$ the corresponding distribution. We obtain an equation for $g_s(m)$ by writing down the formula for the distribution of $m_n^{(\pm)}$ in terms of the identical distribution of $m_{\pm(n+1)}^{(\pm)}$. Using Eq. (7), it is

$$g_s(m) = \int_0^\infty dm' g_s(m') \int_0^\infty dy\, R(y) \times \delta\left[m - \left(\frac{1}{y} + \frac{1}{s/\kappa + m'}\right)^{-1}\right], \tag{8}$$

where we made the variable substitution $y = 1/\xi$, with $R(y) = \varrho(1/y)/y^2$ denoting the corresponding distribution. The function $\delta(z)$ is the Dirac delta-function. Eq. (8) constitute an integral equation for $g_s(m)$.

The probability density for the mobility (in Laplace space) is obtained by integrating over all m's and y's consistent with Eq. (6):

$$P[\hat{\mu}_0(s)] = \int_0^\infty dy\, R(y) \int_0^\infty dm\, g_s(m) \int_0^\infty dm' g_s(m') \times \delta\left[\hat{\mu}_0(s) - \left(\frac{1}{y} + \frac{1}{s/\kappa + m} + \frac{1}{s/\kappa + m'}\right)^{-1}\right]. \tag{9}$$

Equations (8) and (9) define the problem to be solved. In the following we give asymptotically exact results for $s \to 0$ (long times), from which heterogeneity averages can be calculated.

A. LT systems

Let us first give the results for the quantity of interest, i.e., the tracer particle mobility probability density [Eq. (9)], for LT systems. We make use of the explicit expression for $g_s(m)$ contained in Eqs. (A1), (A4), and (A5) in Appendix A and find, for $s \to 0$, that

$$P[\hat{\mu}_0(s)] = \delta[\hat{\mu}_0(s) - \hat{\mu}_0(s)|_{\mathrm{EM,LT}}], \tag{10}$$

where

$$\hat{\mu}_0(s)|_{\mathrm{EM,LT}} \sim \frac{s^{1/2}}{2(\kappa\bar{\xi})^{1/2}}. \tag{11}$$

From Eqs. (10) and (11) we see that LT systems behave universally at long times like a system of identical particles all having the friction constant equal to the mean $\bar{\xi}$.

The result for the tracer particle mobility contained in Eq. (11) is identical to the effective medium mobility obtained in [16] (Appendix A) for LT systems. This effective medium approximation consists of replacing the disordered quantity ξ_n with an n-independent but instead time-dependent friction kernel $\xi_{\mathrm{eff}}(t)$ in such a way that the mobility of a particle on average is unchanged if its effective friction $\xi_{\mathrm{eff}}(t)$ is replaced by one of the original ξ_n. This procedure is thus exact for LT systems at long times.

B. HT systems

For the case of HT systems, i.e., friction constants drawn from a distribution with a heavy power-law tail as described by Eq. (2), the analysis is more challenging. As for LT systems, the problem is divided into two steps, namely, first, solve Eq. (8) and, second, use the corresponding solution for $g_s(m)$ to evaluate Eq. (9).

Considering the first step above, we note that if we choose the specific type of power-law probability density, $R(y) = \alpha y^{\alpha-1}$ for $0 < y < 1$, with $y = 1/\xi$ and $R(y) = 0$ otherwise, Eq. (8) can be solved following the approach in the appendix of Ref. [29] for long times, $s \to 0$ (see also Ref. [30]). In Appendix A we generalize, and simplify, the derivation in [29] to friction constant probability densities of a general type with an asymptotic behavior as in Eq. (2).

Let us now turn to the second step, i.e., evaluating Eq. (9) using the explicit result for $g_s(m)$ obtained in Appendix A. In the limit of $s \to 0$, Eq. (9) becomes (after a rescaling of the integration variable)

$$P[\hat{\mu}_0(s)] = \int_0^\infty dp\, h(p) \int_0^\infty dp' h(p') \times \delta\left(\hat{\mu}_0(s) - \frac{\epsilon(s)}{1/p + 1/p'}\right), \tag{12}$$

where the scaling functions $\epsilon(s)$ and $h(q)$ are related to $g_s(m)$ by $g_s(m) = h[m/\epsilon(s)]/\epsilon(s)$, with expressions for them provided by Eqs. (A11) and (A13). In arriving at Eq. (12) we have made use of the normalization condition $\int_0^\infty R(y)dy = 1$. Taking the Mellin transform with respect to $\hat{\mu}_0(s)$ of Eq. (12), we find

$$\bar{P}[z] = M[P(\mu)] = \int_0^\infty \mu^{z-1} P(\mu) d\mu = [\epsilon(s)]^{z-1} \int_0^\infty dp\, h(p) \int_0^\infty dp' g(p') f(p'/p), \tag{13}$$

where $g(q) = q^{z-1}h(q)$ and $f(q) = (1+q)^{1-z}$. Using Parseval's relation for Mellin transforms and other standard Mellin-transform relations [see Ref. [31], Mellin-transform table, Eqs. (1.3) and (2.17)] and interchanging the order of integrations, we find

$$\bar{P}(z) = \left(\frac{\beta}{\Gamma(\beta)}\right)^2 \frac{B^{z-1}}{\Gamma(z-1)} \int_{c-i\infty}^{c+i\infty} dw\, \bar{G}(1-w)\bar{F}(w), \tag{14}$$

where $\bar{G}(w) = \Gamma(\beta w)\Gamma(\beta z - \beta w)$ and $\bar{F}(w) = \Gamma[\beta(z-2) + \beta w]\Gamma(2\beta - \beta w)$, with $B = B(s) = Q(\beta)\mu_0(s)|_{\mathrm{EM,HT}}$. We define the exponent

$$\beta = 1/(1+\alpha) \tag{15}$$

and introduce the result for the mobility within the effective medium approximation for HT systems [16]:

$$\hat{\mu}_0(s)|_{\mathrm{EM,HT}} \sim \frac{s^\beta}{2(\kappa\chi)^{1/2}}, \tag{16}$$

with $\chi = (4\kappa)^{2\beta-1}(A\pi/\sin[(1-\beta)\pi/\beta])^{2\beta}$. Also,

$$Q(\beta) = \left(\frac{4(1-\beta)}{\beta^3}\Gamma((1-\beta)/\beta)\right)^\beta. \tag{17}$$

In order to arrive at Eq. (14) we also used the reflection formula for Γ functions [32]. Using Parseval's relation in reverse together with standard Mellin transforms [see Ref. [31], inverse Mellin-transform table, Eq. (5.36)], we obtain $\bar{P}(z) = [\Gamma(\beta z)/\Gamma(\beta)]^2 B^{z-1} I/\Gamma(z-1)$, with $I = \int_0^\infty dx(1+x^{1/\beta})^{-2\beta z} x^{z-2}$. Performing the integral I, we get our final expression for the Mellin transform of the tracer particle mobility probability density for HT systems:

$$\bar{P}[z] = \int_0^\infty \mu^{z-1} P(\mu) d\mu = \frac{\beta}{\Gamma(\beta)^2} \frac{B(s)^{z-1}}{\Gamma(z-1)} \frac{\Gamma(\beta z)^2 \Gamma(\beta(z-1))\Gamma(\beta(z+1))}{\Gamma(2\beta z)}. \tag{18}$$

The inverse Mellin transform of $\bar{P}(z)$ is an H function [33]. However, due to the definition of the Mellin transform, Eq. (18) allows us to directly obtain moments of the probability distribution $P[\hat{\mu}_0(s)]$; that is, we have

$$\langle[\hat{\mu}_0(s)]^n\rangle = \bar{P}(n+1). \tag{19}$$

Unlike LT systems, we note that the mobility in the HT systems does not self-average at long times (small Laplace frequencies); that is, the system does not become universal with a δ-peaked distribution of mobilities [compare to Eq. (10)]. This follows since $\langle[\hat{\mu}_0(s)]^n\rangle$ is not simply an n-independent quantity to the power n. Also, in contrast to LT systems, the effective medium prediction for the mean mobility is not exact.

IV. MEAN SQUARE DISPLACEMENT

The results from the previous section allow us to extract the tracer particle mean square displacement. Employing the fluctuation-dissipation theorem [26] in the form of a generalized Einstein relation,

$$\langle \delta x_T(t) \rangle_f = \frac{F_0}{2k_B T} \langle \delta x_T^2(t) \rangle, \tag{20}$$

where the subscript f on the left hand side indicates that the average is performed in the presence of a constant force $f_0(t) = F_0$, whereas the average on the right hand side is in the absence of force. Combining this with Eqs. (18) and (19) for the mean mobility ($n = 1$), we find the heterogeneity-averaged mean square displacement for HT systems:

$$\langle \delta x_T^2(t) \rangle = \Delta(\beta) \frac{k_B T}{(\kappa \chi)^{1/2}} \frac{t^{1-\beta}}{\Gamma(2-\beta)}, \tag{21}$$

where we have introduced a correction factor compared to the effective medium result obtained in [16]:

$$\Delta(\beta) = Q(\beta) \frac{\beta}{\Gamma(\beta)} \frac{[\Gamma(2\beta)]^2 \Gamma(3\beta)}{\Gamma(4\beta)}. \tag{22}$$

The inset in Fig. 2 displays the quantity $\Delta(\beta)$ for the full range of β values. We notice that the effective medium approximation gives the correct exponent $1 - \beta = \alpha/(1+\alpha)$ for the heterogeneity-averaged case, while the corresponding prefactor is not exact.

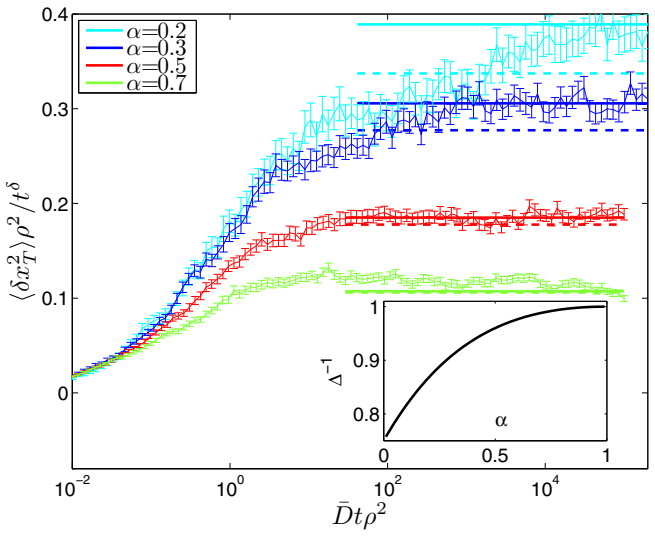

FIG. 2. (Color online) Tracer particle mean square displacement for the heterogeneity-averaged case: comparison of simulations with the effective medium (dashed lines) and exact (solid lines) long time results, Eq. (21). The simulation results are averaged over 2400 realizations with the center particle taken as the tracer particle. The system size is $L = 10\,001$ with $N = 1001$ particles. The rest of the parameters are as given in Sec. V. The inset shows the ratio Δ^{-1} [see Eq. (22)] of the effective medium and exact results for the mean squared displacement of a tracer particle in a HT single-file system as a function of α [see Eq. (2)]. Simulation data for $\alpha = 0.3, 0.5$, and 0.7 are from [16].

V. SIMULATIONS

In this section we provide simulation results in order to numerically test the analytic prediction from the previous two sections.

The simulation scheme employed here is identical to the one described in Appendix G of [16]. Briefly, each particle is placed randomly on a line of length L. The particles make random jumps with a rate $q_n = 2k_B T/(\xi_n a^2)$ and distance l according to the Gaussian distribution $P(l) = (2\pi a^2)^{-1/2} \exp[-(l-\mu)^2/(2a^2)]$. In our simulations we use $a = 1$. The average is set to $\mu = 0$ for all particles except the tagged particle when an oscillating force is applied to it. In this case $\mu = [F_0/(\xi_0 q_0)] \cos(\omega_0 t)$ for a force $f_n(t) = \delta_{n,0} F_0 \cos(\omega_0 t)$. The particles are hard core, interacting with a size of b taken to be unity in the simulations; if an attempted jump would lead to two particles overlapping or crossing, then either the jump is canceled, or both particles are moved according to an algorithm that preserves a detailed balance (see [16] for details). Any jump that would lead to the particle moving outside the system size L is canceled. The distribution of friction constants is taken to be $\varrho(\xi_n) = A \xi_n^{-1-\alpha}$ for $\xi_n \geqslant \xi_c$, $\xi_c = (A/\alpha)^{1/\alpha}$ and zero otherwise, with A chosen such that the average diffusion constant $\bar{D} = \langle k_B T/\xi_n \rangle = \alpha k_B T/[(1+\alpha)\xi_c]$ is unity.

Let us first consider results for the tracer particle mean square displacement (MSD). In Fig. 2 we show a comparison of simulations with the analytical prediction for HT systems [solid lines; Eq. (21)], showing satisfactory agreement and improving previous effective medium predictions (dashed lines). The correction factor for HT systems $\Delta(\beta)$ is shown in Fig. 2 (inset) as a function of the friction-constant exponent α. We see that the effective medium prediction becomes exact as α approaches 1 and deviates at most by 25% in the limit $\alpha \to 0$. For LT systems the fluctuation-dissipation theorem

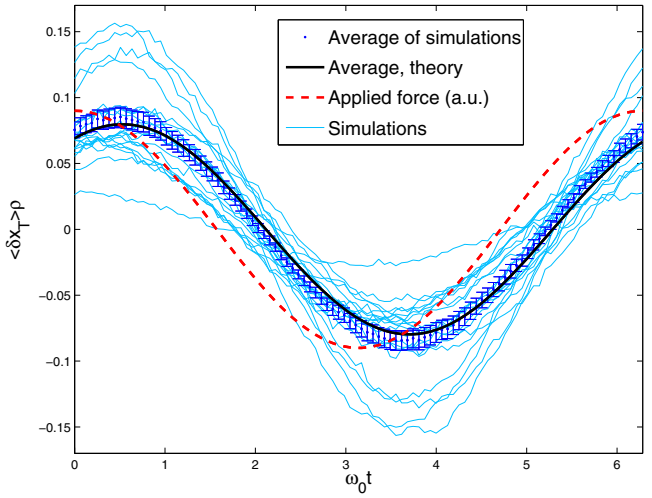

FIG. 3. (Color online) Simulation results for the mean displacement from nonaveraged simulations for 20 HT systems with $\alpha = 0.5$. Also shown are the average of the 20 simulations compared to the result obtained from Eq. (18). We used 501 particles in a box of length 5001 and an oscillation frequency $\omega_0/(2\pi) = 10^{-5}$ and amplitude $F_0/(\xi_0 q_0) = 0.002$.

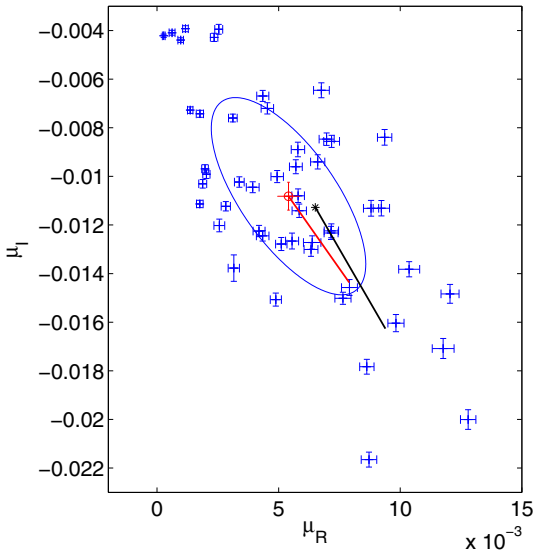

FIG. 4. (Color online) Scatterplot in the complex plane (real axis placed horizontally) of mobilities extracted from 50 nonaveraged simulations (see also Fig. 3, where results for 20 of them are shown). The circle (with error bars) indicates the mean of the extracted mobilities, whereas the asterisk indicates the mean as obtained from Eqs. (18) and (19) with $n = 1$ and $s = -i\omega_0$. The ellipse represents the estimated covariance matrix, with the semimajor and semiminor axes having lengths equal to the square root of the eigenvalues and pointing along the corresponding eigenvectors. The red (gray) line along the major axis has a length equal to the square root of the difference of the eigenvalues. The black line emanating from the asterisk is the analytic result for this line as obtained in Appendix B.

combined with Eq. (10) proves that the effective medium prediction for the MSD in [16] is exact for such systems.

In Fig. 3 we display simulations for the mean displacement in the presence of an oscillating force on the tagged particle $f_0(t) = F_0 \cos(\omega_0 t)$ for HT systems. Due to the nonuniversality of HT systems each realization of friction constants gives a different amplitude and phase for the oscillations around the mean position. The mean value as obtained with the average mobility ($n = 1$) from Eqs. (18) and (19) shows satisfactory agreement with the simulations. Note the phase shift, $(1 - \beta)\pi/2$, between the applied force and the induced response in terms of the mean position. The mobility as extracted from simulations is a complex quantity with real part μ_R and imaginary part μ_I. The theoretical prediction for the mean of μ_R and μ_I is obtained from Eqs. (18) and (19) by setting $n = 1$ and making a Wick rotation $s = -i\omega_0$. To assess the variability around the mean mobility Fig. 4 displays a scatterplot of complex valued mobilities $\mu_{0,m}(\omega_0)$, $m = 1, \ldots, M$, as extracted from simulations of $M = 50$ different sets of frictions by

$$\mu_{0,m}(\omega_0) = -\frac{2i\omega_0}{F_0 N} \sum_{r=1}^{N} e^{i\omega_0 t_r} < \delta x_{T,m}(t_r) >_{\rm sim} , \qquad (23)$$

where $\delta x_{T,m}$ are deviations from the average position for the friction constant set m, t_r runs over equally spaced times within one period of the force, and $< \ldots >_{\rm sim}$ represents an average over different periods within one set of friction constants. The average squared mobility estimated over the 50 different sets of frictions is $\langle \mu_0(\omega_0)^2 \rangle_{\rm sim} = [-(9.4 \pm 1.7) - (13.4 \pm 2.4)i] \times 10^{-5}$, in satisfactory agreement with the corresponding analytic result $\langle \mu_0(\omega_0)^2 \rangle = (-10.1 - 17.6i) \times 10^{-5}$ obtained from Eqs. (18) and (19) with $n = 2$ and $s = -i\omega_0$.

VI. CONCLUSION

Exactly solvable many-body models have, over the years, served all fields of physics, chemistry, and biological sciences. The present article provides important insights into the combined effects of heterogeneity and particle-particle interactions on the dynamics in stochastic processes. In particular, we provided an asymptotically exact analytic expression for the probability density of mobility in a single-file system and for harmonically coupled beads with different friction constants. Our study paves the way for force response studies of other complex heterogeneous many-body systems.

We hope that the type of system introduced here will find experimental realizations for transport processes where heterogeneity is prominent; examples include motion of fluorescently labeled proteins on DNA molecules and other macromolecules and diffusion of dissimilar particles in nanochannels.

ACKNOWLEDGMENTS

T.A. acknowledges funding from the Knut & Alice Wallenberg Foundation and the Swedish Research Council (Grant No. 2009-2924). Computer time was provided by the Danish Center for Scientific Computing.

APPENDIX A: ASYMPTOTIC SOLUTION OF EQ. (8)

Let us consider the expression for the distribution $g_s(m)$, Eq. (8) in the main text, for the case of long times ($s \to 0$). In this limit Eq. (8) can be solved following the approach in the appendix of Ref. [29]. However, as this derivation is lengthy, we here provide a simpler as well as more general version of the derivation. Following Ref. [29], we write

$$g_s(m) = \frac{1}{\epsilon(s)} h[m/\epsilon(s)], \qquad (A1)$$

with the s-dependent scaling function $\epsilon = \epsilon(s)$ chosen to be positive and to satisfy $\epsilon(s) \to 0$ and $s/\epsilon(s) \to 0$ as $s \to 0$. Taking the Mellin transform $[\bar{A}(z) = \int_0^\infty x^{z-1} A(x) dx]$ of Eq. (8) with respect to m and substituting the integration variable with $v = m'/\epsilon$, we get

$$\bar{h}(z) = \int_0^\infty dv\, h(v) \int_0^\infty dy\, R(y) \left(\frac{\epsilon}{y} + \frac{1}{v + s/(\kappa\epsilon)} \right)^{1-z}, \qquad (A2)$$

which is the starting point of our simplified derivation.

1. LT systems

Let us first consider LT systems. For these we expand the right hand side of Eq. (A2) to first subleading order in ϵ and $s/(\kappa\epsilon)$. Also making use of the definition of a Mellin transform, we get that the

right hand side equals $\bar{h}(z) - (1-z)(s/\kappa\epsilon)\bar{h}(z-1) + (1-z)\langle y^{-1}\rangle\epsilon\bar{h}(z+1)$. Equation (A2) then becomes

$$\frac{s}{\kappa\bar{\xi}\epsilon^2}\bar{h}(z-1) = \bar{h}(z+1). \tag{A3}$$

We obtain a nontrivial solution for $\bar{h}$ by choosing

$$\epsilon(s) = \left(\frac{s}{\kappa\bar{\xi}}\right)^{1/2}, \tag{A4}$$

where $\bar{\xi} = \int_0^\infty (1/y)R(y)dy = \int_0^\infty \xi\varrho(\xi)d\xi$ is the mean friction constant. The solution to Eq. (A3) with $\bar{h}(1) = 1$ (normalization condition) is simply $\bar{h}(z) = 1$, which, when Mellin inverted, gives

$$h(x) = \delta(x-1), \tag{A5}$$

in agreement with [29].

2. HT systems

For HT systems the analysis is slightly more involved. First we integrate Eq. (A2) by parts, introducing the cumulative distribution $C(y) = \int_0^y R(y')dy'$, to find $\bar{h}(z) = T_1 + T_2$, with

$$T_1 = \int_0^\infty dv\, h(v)C(y)\left[\frac{\epsilon}{y} + \frac{1}{v + s/(\kappa\epsilon)}\right]^{1-z}\Bigg|_{y=0}^{\infty} \tag{A6}$$

$$T_2 = \int_0^\infty dv\, h(v)\int_0^\infty dy\frac{(1-z)\epsilon}{y^2}C(y)\left[\frac{\epsilon}{y}+\frac{1}{v+s/(\kappa\epsilon)}\right]^{-z}. \tag{A7}$$

Since $R(y) \sim A/y^{1-\alpha}$ for small y, we have $C(y) \sim Ay^\alpha/\alpha$. Restricting z to $z > 1-\alpha$, the lower boundary term above vanishes. At the opposite boundary we have $C(\infty) = 1$, and thus we get

$$T_1 = \int_0^\infty dv h(v)v^{z-1}\left[1 + \frac{s}{\kappa\epsilon v}\right]^{z-1}. \tag{A8}$$

For T_2, if we set $y = \epsilon y'$ and let $\epsilon \to 0$, we have $C(\epsilon y') \sim A(\epsilon y')^\alpha/\alpha$ and find, to leading order in ϵ and s/ϵ,

$$\begin{aligned} T_2 &\sim \int_0^\infty dv\, h(v)\int_0^\infty dy'\frac{(1-z)}{(y')^2}\frac{A(\epsilon y')^\alpha}{\alpha}\left[\frac{1}{y'}+\frac{1}{v}\right]^{-z} \\ &= \epsilon^\alpha\frac{A(1-z)\Gamma(1-\alpha)\Gamma(z+\alpha-1)}{\alpha\Gamma(z)}\bar{h}(z+\alpha). \end{aligned} \tag{A9}$$

Similarly, we expand T_1, but here we include the subleading term in $s/(\kappa\epsilon)$,

$$T_1 \sim \bar{h}(z) + \frac{(z-1)s}{\kappa\epsilon}\bar{h}(z-1). \tag{A10}$$

From Eqs. (A9) and (A10) we see that a way to obtain a nontrivial equation for $\bar{h}(z)$ in the limit $s \to 0$ is to choose

$$\epsilon(s) = \left(\frac{\alpha s}{\kappa A}\right)^\beta, \tag{A11}$$

with $\beta = 1/(1+\alpha)$. With this choice we find that $\bar{h}(z)$ satisfies

$$\bar{h}(z-1) = \frac{\Gamma(z+\alpha-1)\Gamma(1-\alpha)}{\Gamma(z)}\bar{h}(z+\alpha), \tag{A12}$$

which has the solution [with $\bar{h}(1) = 1$]

$$\bar{h}(z) = \frac{\beta}{\Gamma(\beta)}[\beta^2\Gamma(1-\alpha)]^{\beta(1-z)}\frac{\Gamma(\beta(z-1))\Gamma(\beta z)}{\Gamma(z-1)}, \tag{A13}$$

in agreement with [29].

APPENDIX B: THE COVARIANCE MATRIX

Writing the mobility in Fourier space according to (with $\delta\mu_R$ and $\delta\mu_I$ being real)

$$\mu_0(\omega_0) = \langle\mu_0(\omega_0)\rangle + \delta\mu_R + i\delta\mu_I, \tag{B1}$$

we can define a covariance matrix for the real and imaginary deviations:

$$\Sigma = \begin{pmatrix} \langle\delta\mu_R^2\rangle & \langle\delta\mu_R\delta\mu_I\rangle \\ \langle\delta\mu_R\delta\mu_I\rangle & \langle\delta\mu_I^2\rangle \end{pmatrix}. \tag{B2}$$

From simulation data with estimates $\mu_{0,m}(\omega_0)$, $m = 1,\ldots,M$, of mobility from M different sets of friction coefficients we estimate the average as $\langle\mu_0(\omega_0)\rangle_{\text{est}} = \sum_{m=1}^M \mu_{0,m}(\omega_0)/M$. For the deviations $\delta\mu_{R,m} + i\delta\mu_{I,m} = \mu_{0,m}(\omega_0) - \langle\mu_0(\omega_0)\rangle_{\text{est}}$ we estimate the components of Σ by

$$\langle\delta\mu_A\delta\mu_B\rangle_{\text{est}} = \frac{1}{M-1}\sum_{m=1}^M \delta\mu_{A,m}\delta\mu_{B,m}, \tag{B3}$$

where A and B are either R or I. The ellipse in Fig. 3 has been drawn with its center on $\langle\mu_0(\omega_0)\rangle_{\text{est}}$ and with the major and minor radii equal to the square roots of the eigenvalues of the estimated Σ. The corresponding axes point along the eigenvectors.

The analytic result for the second moment about the mean, $\langle(\delta\mu_R + i\delta\mu_I)^2\rangle$, allows us to extract two results regarding the covariance matrix Σ. One regards its eigenvalues $\lambda_\pm$,

$$\lambda_\pm = \frac{\langle\delta\mu_R^2\rangle + \langle\delta\mu_I^2\rangle \pm \sqrt{\left(\langle\delta\mu_R^2\rangle - \langle\delta\mu_I^2\rangle\right)^2 + 4\langle\delta\mu_R\delta\mu_I\rangle^2}}{2}. \tag{B4}$$

The difference of these can be found from the analytic calculation of the moments as

$$\begin{aligned} \lambda_+ - \lambda_- &= \sqrt{\left(\langle\delta\mu_R^2\rangle - \langle\delta\mu_I^2\rangle\right)^2 + 4\langle\delta\mu_R\delta\mu_I\rangle^2} \\ &= |\langle(\delta\mu_R + i\delta\mu_I)^2\rangle| \\ &= |\langle\mu_0(\omega_0)^2\rangle - \langle\mu_0(\omega_0)\rangle^2|. \end{aligned} \tag{B5}$$

Note that Eq. (B5) implies that $\lambda_+ \geqslant \lambda_-$. We can also extract the eigenvectors. To see this first note that the asymptotic result $\langle\mu_0(\omega_0)^n\rangle \simeq (-i\omega_0)^{n\beta}$ for the nth moment tells us that $\langle(\delta\mu_R + i\delta\mu_I)^2\rangle = Ce^{2i\phi}$, where $C > 0$ and $e^{i\phi} = \langle\mu_0(\omega_0)\rangle/|\langle\mu_0(\omega_0)\rangle|$; that is, the phase of the second moment is twice that of the first moment. Using this, we find that the eigenvector corresponding to λ_+ is

$$\begin{aligned} \vec{v}_+ &= \begin{pmatrix} \langle\delta\mu_R\delta\mu_I\rangle \\ \lambda_+ - \langle\delta\mu_R^2\rangle \end{pmatrix} = \frac{C}{2}\begin{pmatrix} \sin 2\phi \\ 1 - \cos 2\phi \end{pmatrix} \\ &= C\sin\phi\begin{pmatrix}\cos\phi\\ \sin\phi\end{pmatrix} = \frac{C\sin\phi}{|\langle\mu_0(\omega_0)\rangle|}\begin{pmatrix}\text{Re}\,\langle\mu_0(\omega_0)\rangle\\ \text{Im}\,\langle\mu_0(\omega_0)\rangle\end{pmatrix}. \end{aligned} \tag{B6}$$

Thus, for the ellipse plotted in Fig. 3 of the main text we find that the major axis should point along the line to the origin. The black line in Fig. 3 drawn from the asterisk has a length $\sqrt{\lambda_+ - \lambda_-}$ and points along $-\vec{v}_+$, as obtained from the analytic results.

[1] R. Kubo, Science **233**, 330 (1986).
[2] U. M. B. Marconi, A. Puglisi, L. Rondini, and A. Vulpiani, Phys. Rep. **461**, 111 (2008).
[3] C. Bustamante, Y. R. Chemla. N. R. Forde, and D. Izhaky, Annu. Rev. Biochem. **73**, 705 (2004).
[4] C. Jarzynski, Phys. Rev. Lett. **78**, 2690 (1997).
[5] M. Gorissen, A. Lazarescu, K. Mallick, and C. Vanderzande, Phys. Rev. Lett. **109**, 170601 (2012).
[6] T. E. Harris, J. Appl. Probab. **2**, 323 (1965).
[7] M. Kollmann, Phys. Rev. Lett. **90**, 180602 (2003).
[8] F. Marchesoni and A. Taloni, Phys. Rev. Lett. **97**, 106101 (2006).
[9] E. Barkai and R. Silbey, Phys. Rev. Lett. **102**, 050602 (2009).
[10] C. Aslangul, J. Phys. A **33**, 851 (2000).
[11] A. Brzank and G. M. Schütz, J. Stat. Mech. Theor. Exp. (2007) P08028.
[12] P. Goncalves and M. D. Jara, J. Stat. Phys. **132**, 1135 (2008).
[13] M. Jara, arXiv:0901.0229.
[14] T. Ambjörnsson, L. Lizana, M. A. Lomholt, and R. J. Silbey, J. Chem. Phys. **129**, 185106 (2008).
[15] O. Flomenbom, Phys. Rev. E **82**, 031126 (2010).
[16] M. A. Lomholt, L. Lizana, and T. Ambjörnsson, J. Chem. Phys. **134**, 045101 (2011).
[17] V. Kukla, J. Kornatowski, D. Demuth, I. Girnus, H. Pfeifer, L. Rees, S. Schunk, K. Unger, and J. Kärger, Science **272**, 702 (1996).
[18] T. Meersmann, J. W. Logan, R. Simonutti, S. Caldarelli, A. Comotti, P. Sozzani, L. G. Kaiser, and A. Pines, J. Phys. Chem. A **104**, 11665 (2000).
[19] K. Hahn, J. Kärger, and V. Kukla, Phys. Rev. Lett. **76**, 2762 (1996).
[20] Q. H. Wei, C. Bechinger, and P. Leiderer, Science **287**, 625 (2000).
[21] V. Gupta, S. S. Nivarthi, A. V. McCormick, and H. T. Davis, Chem. Phys. Lett. **247**, 596 (1995).
[22] A. L. Hodgkin and R. D. Keynes, J. Physiol. **128**, 61 (1955).
[23] K. C. Vermeulen, G. J. Stienen, and C. F. Schmid, J. Muscle Res. Cell Motil. **23**, 71 (2002).
[24] F. Berger, C. Keller, S. Klumpp, and R. Lipowsky, Phys. Rev. Lett. **108**, 208101 (2012).
[25] G.-W. Li, O. G. Berg, and J. Elf, Nat. Phys. **5**, 294 (2009).
[26] R. Kubo, Rep. Prog. Phys. **29**, 255 (1966).
[27] L. Lizana, T. Ambjörnsson, A. Taloni, E. Barkai, and M. A. Lomholt, Phys. Rev. E **81**, 051118 (2010).
[28] The analysis performed here is similar to the one in Appendix A of Ref. [16] (in Laplace space rather than in the Fourier domain). The relation between our m_n's and the quantities in Ref. [16] is $m_n^{(\pm)}(s) = [\xi_n + \gamma_n^{(\pm)}(s)]^{-1}$.
[29] J. Bernasconi, W. R. Wyss, and W. Wyss, Z. Phys. B **37**, 175 (1980).
[30] S. Alexander, J. Bernasconi, and W. R. Schneider, Rev. Mod. Phys. **53**, 175 (1981).
[31] F. Oberhettinger, *Tables of Mellin Transforms* (Springer, New York, 1974).
[32] M. Abramowitz and I. A. Stegun, *Handbook of Mathematical Functions with Formulas, Graphs, and Mathematical Tables* (Dover, New York, 1964).
[33] A. M. Mathai, R. K. Saxena, and H. J. Haubold, *The H-Function: Theory and Applications* (Springer, Berlin, 2010).